Journal Name

ARTICLE

Antisolvent addition at extreme conditions

Martin R. Ward,*[a] Iain D.H. Oswald[a]

Received 00th January 20xx,
Accepted 00th January 20xx

DOI: 10.1039/x0xx00000x

www.rsc.org/

This article describes the use of antisolvent addition at high-pressure to aid precipitation and recovery of high-pressure phases to ambient pressure. Paracetamol (PCM) was used as a model system to demonstrate the principle due to the extensive literature of paracetamol at high-pressure and ambient pressure. We have observed that we are able to recover the orthorhombic form of paracetamol to ambient pressure using this technique, although solvent-mediated transformations are a hurdle. During this investigation we observed a new methanol solvate of paracetamol that is simlar in structure to the known form. The methanol solvate is stable to 0.2 GPa before transformation to the orthorhombic form that is known to be the stable form at high pressure.

Introduction

Exploring the solid-state landscape and the discovery of new solid forms is a continual challenge in the field of solid-state science. The motivation behind this is that a new or alternative solid form, even polymorphs, can display markedly different physical properties. The objective of tuning physical properties of a material is of particular importance in the pharmaceutical industry where deriving a new form of a drug can provide improved properties for processing or improved solubility e.g. Form II of paracetamol (PCM) compared to Form I (that is typically produced at ambient conditions).

High-pressure studies have been shown to be a highly effective route to the discovery of new polymorphs,[1,2] the observation of metastable solid forms;[3] and the relative stability of polymorphs at pressure and in presence of seeds.[4] The role of kinetic transformations between polymorphs of materials have been explored in serine[5] and chlorpropamide.[4] Chemical transformations and reactions have been explored such as dehydration[6] or polymerisation.[7–10] Traditionally, these studies utilise a diamond anvil cell (DAC) to provide a high-pressure environment (~0.1-100's GPa) with the sample crystal monitored by single crystal X-ray diffraction (SC-XRD) during compression/decompression.[11–14]

Alternatively, the DAC has also been used to perform crystallization at high-pressure by loading a solution sample and taking advantage of a typical decrease in solute solubility as pressure is increased.[15,16] By this method crystal formation occurs at high-pressure conditions rather than inducing a solid-state transformation by the application of pressure. For a number of systems, the process of in-situ nucleation under high-pressure conditions has been shown to provide access to a high-pressure solid phase at significantly lower pressures than required to observe the pressure-induced transformation to a high pressure form.[3,17,18] Due to the dimensions of the sample chamber (ca. 200 µm diameter, 90 µm thick) in the DAC assembly, these studies are limited by the quantity of crystallised solute and rely on spectroscopy (in-house), powder X-ray diffraction at synchrotron facilities or single crystal measurements through annealing of the powder into a single crystal. Attempts to recover phases have been made successfully and used to seed ambient pressure crystallisations.[19,20]

High-pressure studies can be performed in significantly greater volumes using a large volume press (LVP) assembly. Rather than single crystal quantities of materials, the LVP can accommodate 100's-1000's mg sample.[3,10,20] A drawback of the LVP is that the sample chamber is completely enclosed during the experiment and therefore restricts analysis of the sample to ex-situ measurements in a home laboratory. Larger volumes can be accommodated on the beamline at Central Facilities using the Paris-Edinburgh press[21,22] and these have been used successfully to explore molecular systems to high-pressure on a larger scale.[10,23–29]

In the present work, (see Table S4) we have selected the model system of paracetamol to investigate use of antisolvent addition crystallization at high-pressure conditions. Successful demonstration of antisolvent addition at high-pressure would present a new approach to solid form discovery at extreme conditions and would hopefully stimulate further interest in the use of high-pressure methods for solid form discovery.

Methods

Paracetamol solutions

To ensure sufficient solids were precipitated during an antisolvent addition crystallization, a solvent system was

[a] Strathclyde Institute of Pharmacy & Biomedical Sciences (SIPBS), University of Strathclyde, 161 Cathedral Street, Glasgow, G4 0RE, UK.
Email: martin.ward@strath.ac.uk, iain.oswald@strath.ac.uk

†Electronic Supplementary Information (ESI) available: [details of any supplementary information available should be included here]. See DOI: 10.1039/x0xx00000x

selected with high solubility of PCM that also decreases rapidly with the addition of the anti-solvent. In addition to this criterion, the solubility of the PCM with pressure was a consideration as we did not want the solution to precipitate out with pressure alone. To assess this, we applied pressure to three different concentrations of solution, 0.05, 0.1 and 0.2 g/g PCM/solvent. Based on the solubility determinations of PCM in binary aqueous solvent systems by Ó'Ciardhá C et. al.[30] a mixture of Methanol:water (MeOH:H_2O)(64 % w/w MeOH) was selected for this work. For high-pressure antisolvent addition experiments the same sample concentrations were prepared. Paracetamol was purchased from Sigma Aldrich (Sigma BioExtra ≥ 99.0%, A7085) and used as received. An appropriate amount of PCM was weighed out in to a 100 mL duran bottle to which a corresponding amount of solvent mixture was added. Complete dissolution was ensured by sonication of the sample bottle in a warm (40 °C) water bath with the samples allowed to cool back to room temperature before further use.

Diamond Anvil Cell

A Merrill-Bassett Diamond anvil cell was used for the initial screening of the precipitation process from solution. Gem quality diamonds with 600 µm culets were used together with a piece of tungsten foil with a 250 µm hole to serve as the sample chamber. Pressure measurements were made using the ruby fluorescence method.[31] In three different experiments, solutions of 0.05, 0.10 and 0.20 g/g PCM/solvent were added to the DAC and sealed before applying pressure. In each experiment, ~0.8 GPa of pressure was applied to the solution (maximum pressure of Large Volume Press) and the sample left at this pressure for ca 2 hours; this was to address the challenge of pressure-induced nucleation. For all tested concentrations, no precipitation was observed on compression to 0.8 GPa nor over a timescale of at least 2 hours with some samples monitored for longer periods (0.05g/g 48 hours). Whilst the size of the chamber in the DAC is very much smaller than the large volume press, this was the only method by which the precipitation could be viewed microscopically hence allowing us to mitigate the chance of precipitation with pressure alone.

Large volume press

High-pressure conditions were provided by use of a large volume press assembly. The sample chamber comprised a PTFE tube (ID = 8.0 mm, OD = 10.0 mm) sealed using PTFE end caps and PTFE sealing tape.[20]

The axial compression of the PTFE sample tube during compression (reduction in length) was tested and recorded by video monitoring. The sample chamber was filled with MeOH:H_2O mixture (64:36 w/w) and load applied to the cell incrementally up to a maximum load of 7-ton (equivalent sample pressure ca 0.8 GPa). An identifiable mark was placed on the pneumatic actuator of the press at the relative position and monitored during compression using a Basler acA1920—40uc camera and zoom lens assembly. This information allowed calculation of the length of the PTFE sample tube as a function of applied load hence sample pressure.

For anti-solvent addition, water was used as the antisolvent during this work. A glass ampoule was flame sealed at one end and then filled with deionized water (approx. 1 mL, 18 MΩ cm^{-1}) before sealing the other end with epoxy glue. The glue was allowed to fully cure and harden before further use. To assist with breakage of the antisolvent tube, the walls were scored around its diameter using a ceramic cutting blade at three positions, equidistant, along the tube. The sealed antisolvent tube was placed in the PTFE sample tube before filling the remaining volume of the PTFE tube with the paracetamol solution and sealing into the high-pressure cell. Samples were taken to ca. 0.8 GPa and held at this pressure for approx. 20 minutes. Mixing in the sample chamber was promoted by manually rotating/inverting the high-pressure cell assembly before downloading back to ambient pressure. Any solids produced were isolated by filtration before further analysis by Raman spectroscopy or single crystal X-ray diffraction.

Gravimetric solubility determination

The solubility of PCM in 64% w/w aqueous MeOH solution at the experimental temperature (Room temperature, 20 °C) was determined using gravimetric methods. A solution was prepared with excess PCM in the aqueous MeOH mixture and sealed to equilibrate over 24 hours at 20 °C. Once saturated, the solution was syringe filtered (Millex-GP, 0.22 µm) into pre-weighed vials that were maintained at 20 °C. Samples were loosely covered to prevent ingress of contaminants and to allow loss of solvent through evaporation. Samples were held at a temperature of 20 °C for 8 days before recording vial masses. Masses were subsequently recorded daily to ensure samples were fully dry. Recorded masses stabilised after day 10 of evaporation/drying. All weighing was performed using a Mettler Toledo AG204 analytical balance.

Single crystal X-ray diffraction

Ambient pressure

Single crystal X-ray diffraction (SC-XRD) data were obtained using a Bruker D8 venture diffractometer equipped with a Photon 100 detector and Incoatec microfocus Cu X-ray source ($K\alpha_1$, λ = 1.5406 Å). Data were collected and reduced using Bruker Apex3 software. Resolved structures were solved by intrinsic phasing using SHELXT using Olex2[32] (v1.2) software. Full-matrix least-squares refinement of data was performed with SHELXL using Olex2 software. All non-hydrogen atoms were treated anisotropically. Hydrogen atoms were placed on the carbon atoms and allowed to ride on their parent atoms.

High pressure

SC-XRD data were obtained using a Bruker Apex II diffractometer equipped with an Incoatec microfocus Mo X-ray source ($K\alpha_1$, λ = 0.71073 Å). Data were reduced using Bruker Apex3 software. During the processing of data, it was apparent that the unit cell dimensions (from all three experiments, 0.05, 0.1, 0.2 g/g) were different to those of the paracetamol[33] and paracetamol:methanolate.[34] The structure was solved by intrinsic phasing using SHELXT using Olex2[32] (v1.2) software and the coordinates were subsequently used for each high pressure

dataset. Full-matrix least-squares refinement of data was performed with SHELXL using Olex2 software. All non-hydrogen atoms were treated isotropically due to the paucity of data available from the sample in the diamond anvil cell. The phenyl groups were constrained to be hexagons and the hydrogen atoms were placed on the carbon atoms and allowed to ride on their parent atoms. The hydroxyl hydrogen atoms were ideally placed on the oxygen atoms and allowed to ride.

The solved structure possessed three molecules of paracetamol and three molecules of methanol. Structural comparison with the known methanol solvate (Rint ~5%; R-factor 13.4%)[34] in the database using the packing similarity search in Mercury showed that all 15 molecules were aligned to one another giving a root mean square deviation of 0.551.[35] The similarity in structure forced a significant interrogation of our data to ensure that the correct unit cell and space group were assigned. Through combinations of brute force identification of unit cell (cell_now[36]) together with close inspection of the diffraction data we were unable to identify a cell that matched the previous work. Integration of potential cells (with similar dimensions to the methanolate) resulted in very poor integrations for those unit cell choices. The reduced data from the previous study was provided to us as a private communication but unfortunately the raw frames were not present. From the reduced data and the list files from this experiment it was clear that the choice of cell by the authors was correct. With our interrogation and the knowledge of the previous work we believe that this is another very similar polymorph of the solvate isolated from a different medium. We have used aqueous media in this study so this may be having a nuanced effect on the polymorphism. The data are deposited at the University of Strathclyde KnowledgeBase indicated in the acknowledgements.

X-ray powder diffraction

X-ray powder diffraction (XRPD) measurements were performed on a Bruker D8 Advance II diffractometer configured in Debye-Scherrer transmission geometry. The diffractometer was equipped with a multiwell stage with a single layer of Kapton film to contain the samples. X-ray emission was provided by a Cu source (λ = 1.5406Å) used in conjunction with a Kα1 Johansson monochromator and 1 mm anti-divergence slit. A Vantec 1D detector was used together with 2.5° Soller slits. All data was collected at room temperature without grinding the sample material. Simple Pawley fitting and Rietveld refinement of the XRPD data was performed using Topas (Academic, V5).[37]

Raman spectroscopy

A Horiba Xplora Raman microscope equipped with a 532 nm laser source was used for the collection of Raman spectra. Slit, Hole, Filters and accumulation times were varied to maximise the sample signal and reduce any fluorescence that may have come from the sample environment, however final spectra were the sum of 2 accumulations to account for any transitory events.

UV-vis spectroscopy

UV-vis spectra were collected using a Jenway Genova Nano UV-vis spectrophotometer. Spectra were recorded over 200-400 nm with resolution of 2 nm. Concentrated PCM solutions were diluted with aqueous MeOH (64% w/w MeOH) by a factor of 8000 to provide a suitable signal over the concentration range of samples tested. A calibration curve was constructed using solutions of known concentrations (0.14, 0.18, 0.20, 0.22 and 0.24 g/g solute/solvent). Sample solutions were then tested following the same experimental procedure and dilution factor with all measurements made in triplicate.

Results and Discussion

Large volume press tests

We tested a range of solutions (0.10-0.22 g/g) in the large volume press without the addition of the antisolvent to observe whether the PCM precipitated from solution and was recoverable to ambient pressure without the use of the antisolvent. During these experiments, we noted that samples appeared to undergo a phase separation and showed a clear boundary between two colourless liquid phases inside the PTFE sample tube on recovery to ambient pressure. The phase separation was clearly visible when we inverted the sample tubes. We performed UV experiments on the upper portion of the liquid to calculate its PCM concentration (Table 1). The upper layer of the liquid demonstrates a lower concentration of the solution verifying the visual evidence. Our explanation for this is that over this pressure range the paracetamol precipitates from solution and the solid falls to the bottom of the tube. On decompression to ambient pressure, the precipitate dissolves leading to an apparent liquid/liquid phase separation with a more concentrated solution at the bottom of the tube. Extrapolating this data to lower concentrations allows us to estimate that at 0.05 g/g PCM/solvent, there would be no precipitation at all from direct compression of the solution hence would be ideal to test the antisolvent addition.

Table 1. Summary of UV-vis measurements made on 200 µL aliquots of the upper layer observed following compression of sample solutions to ca 0.8 GPa pressures

Solution concentration (g/g solvent)	Mean absorbance (248 nm)	Calculated concentration (g/g solvent)	% difference to expected concentration
0.14	0.302	0.048	66.0
0.16	0.446	0.070	56.1
0.18	0.631	0.099	44.9
0.20	0.682	0.107	46.4
0.22	0.973	0.153	30.4

Large volume press – antisolvent addition

Anti-solvent addition experiments were performed using water as the antisolvent and an aqueous solution of MeOH (64% MeOH w/w) as the solvent phase. We selected this system based on reported solubility data for PCM that demonstrated both good solubility (ca 100's mg/g solvent) and a significant rate of change of solubility with increasing water content that

would maximise the precipitation of PCM for a given amount of antisolvent delivered to the solution phase.

We used a glass ampoule filled with water to add the antisolvent to the solution. Through systematic evaluation of the compression length in the press we designed the ampoule to break at the point where the target sample pressure was reached, e.g. 0.8 GPa. The nature of the equipment (Copper-Beryllium cell) prevented us from observing the successful breakage of the glass ampoule until the end of the experiment when the sample cell was brought back to ambient pressure. In spite of this, it was found that breakage of the antisolvent ampoule was very reproducible and occurred 9/11 attempts. For each sample that saw breakage of the glass ampoule, crystallization had occurred with the solids recoverable back to ambient pressure when downloaded. The amount of crystallized material would vary from sample to sample that is likely a result of the way in which the antisolvent ampoule had broken and the amount of mixing of the solution and antisolvent that had occurred within the cell. Typically, we observed crystals at the bottom of the PTFE tube and within broken fragments of the antisolvent ampoule. We were able to isolate the crystals from the sample for imaging, Raman spectroscopy and SC-XRD. Samples isolated by filtration would yield between 50-200 mg of material.

A number of particles were tested by Raman spectroscopy to assess the crystal forms present at each location in the sample i.e. the bottom of the PTFE capsule or in the ampoule. Differentiation of the Form I, II polymorphs by Raman spectroscopy was performed by monitoring characteristic peaks[38] over the range 400-525 cm^{-1} e.g. 454, 465 and 504 cm^{-1}. Raman spectra collected for crystals found at the bottom of the PTFE tube and within broken glass fragments during LVP experiments are shown in Figure 1. Crystals that were recovered from inside the fractured glass antisolvent tube were found to be exclusively Form I PCM. In contrast, crystals samples from the bottom of the PTFE tube were found to be a mixture of Form I and II PCM. It is noted, however, that crystals within the broken fragments of glass were difficult to isolate from the solution phase due to contact with the glass fragments. These particles could not be readily filtered and remained in contact with the solution phase for longer, therefore these particles have an increased likelihood of solution-mediated transformation to PCM I.

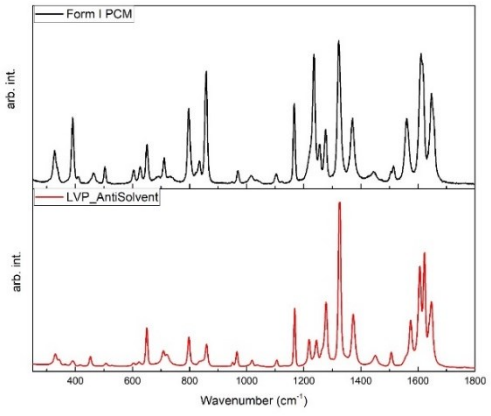

Figure 1. Raman spectra for crystals obtained during antisolvent addition in a large volume press. The spectra for crystals collected from the bottom of the PTFE sample tube (lower, red) are consistent with Form II paracetamol. The spectrum collected for Form I crystals found within the fractured antisolvent ampoule is also shown for reference (upper, black)

A microscope image is shown in Figure 2a and comprises a mixture of well-defined particles of distinct morphologies; the image was collected approximately 30 minutes after the sample was brought back to ambient pressure. Two distinct morphologies are seen throughout the sample mixture - long rods and blocks. These morphologies are those expected for Form II and Form I PCM, respectively.

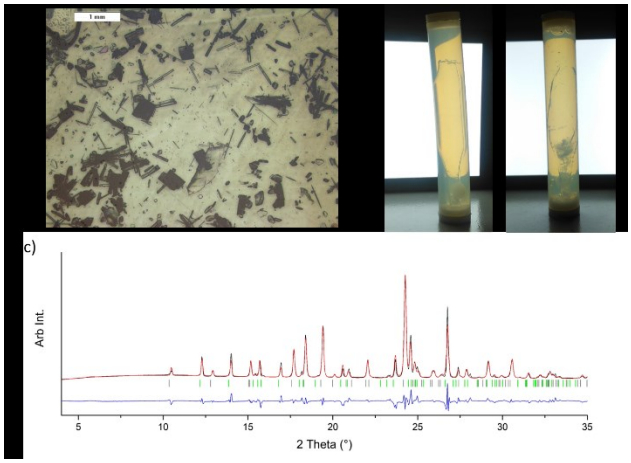

Figure 2: a) Microscopy images of the crystals from the LVP experiments after recovery to ambient pressure showing a mixture of Form I and II PCM crystals. b) The ampoules of PCM solution and antisolvent before (left) and after (right) compression indicating the fracture of the ampoule and crystallisation of PCM. c) The Rietveld fit of PCMI and PCM II to the data from the crystals recovered from the antisolvent high-pressure experiment indicating a mixed phase.

The composition of the crystallized product was tested using XRPD. We rapidly isolated the product through filtration (approx. 10 minutes after download to ambient pressure) before collection of XRPD data. Initially, we emptied the contents on to a filter paper for isolation with all visible fragments of broken glass removed before XRD analysis. The sample w as collected repeatedly (5 times, 35 min per collection) over 3 hours to assess how stable the sample mixture was. Over the 3-hour period, the XRPD pattern remained unchanged and therefore it was established that filtration was sufficient to limit further solid form transformation. A rigid body Rietveld refinement of the XRPD data was performed using reference structures from the CSD (HXACAN04 and HXACAN08), confirming a mixture of Form I and II of PCM with an approximate relative composition of 58% Form II and 42% Form I (Figure 2c).

Table 2. Summary of data obtained from single-crystal X-ray diffraction on a Form II PCM particle obtained through antisolvent addition at high-pressure.

Crystal system, space group	Orthorhombic, *Pbca*
Temperature (K)	296
a, b, c (Å)	17.1522 (5), 11.8201 (4), 7.3985 (2)
V (Å^3)	1499.98 (8)
Z	8
Radiation type	Cu K_α (λ = 1. 540596 Å)
R_{int}	0.038
(sin θ/λ)max (Å^{-1})	0.603
R[$F^2 > 2\sigma(F^2)$], wR(F^2), S	0.045, 0.122, 1.07

We analysed single crystals removed from the sample tube (and ampoule fragments) using single crystal X-ray diffraction to confirm the solid form indicated by initial Raman spectroscopy. All crystals removed from the broken ampoule fragments indexed with unit cell parameters consistent with Form I PCM. Numerous crystals retrieved from the bottom of the PTFE tube were also indexed that indicated a mixture of crystals that indexed with unit cell parameters consistent with Form I and Form II PCM. These observations are in line with the results obtained from Raman spectroscopy measurements on crystals isolated from these distinct regions within the sample cell. The quality of the crystals isolated via this technique is demonstrated by a full collection on a Form II crystal (Table 2. Summary of data obtained from single-crystal X-ray diffraction on a Form II PCM particle obtained through antisolvent addition at high-pressure.).

Mixed phase

The presence of the mixed phase in the tubes is concerning for the control of polymorphism. The formation of Form II PCM may be a direct result of nucleation at elevated pressure. Experiments performed in DAC have reported in-situ nucleation of PCM form II from acetone, dioxane and water solutions at pressures below those achieved during these experiments (~0.4 GPa).[3] Additionally, paracetamol forms a methanol solvate at ~0.6 GPa that may be applicable in this experiment. It is therefore implied that if anti-solvent addition occurs around 0.8 GPa, the resulting product could be Form II PCM or the methanol solvate. Form I PCM produced during these experiments may then result from anti-solvent/solution mixing that occurs during decompression. The potential for solvent mediated transformation of Form II→ Form I PCM is possible and FBRM measurements have been used to study the solution mediated transformation of Form II → Form I PCM in EtOH:MeOH (95:5 v/v) solution in work by Barthe and Grover.[39] Their results showed a rapid transformation over a period of minutes with an apparent complete conversion taking place over a time period ca. 1 hour. In our work, the decompression to ambient pressure and recovery of the crystals for analysis requires approximately 10-20 minutes to complete and therefore it is likely that at least some degree of solution mediated transformation of Form II → Form I PCM has occurred prior to sample analysis. During microscopy of a sample prepared during this study a series of images were recorded over a 30-minute period with the crystals in contact with the solution phase that showed the growth of Form I crystals at the expense of Form II crystals that dissolved back in to solution. These crystals were first imaged approximately 30 minutes after download back to ambient pressure and then monitored for a further 30 minutes (Figure S4). Problems associated with recovery of PCM II back to ambient pressure have also been reported by Oswald et al where it was found that cooling the sample to 275-280 K significantly reduced the rate of solution mediated transformation to PCM I.[3] In the present work, cooling of the sample chamber during compression/decompression in the home laboratory was not a viable option. As an alternative, one test was performed in which 0.5 mL of perfluorinated oil (Perfluoropolyether fluid, Galden SV110, Solvay, Italy) was included in the PTFE tube before filling with PCM solution. On download back to ambient pressure, the sample had crystallized and the resultant solids were isolated at the interface between the oil and solution phases. Rietveld refinement of the XRPD data indicate an increased proportion (65%) of PCM II in the sample mixture when using oil compared to without oil (58 %). This is taken as an indication of the role of solution mediated transformation of PCM during sample download and isolation prior to analysis.

We also cannot rule out a gradient of supersaturation during the experiment. Sudha and Srinivasan have reported the supersaturation dependence of nucleation of Form I and II PCM and have shown that nucleation of Form I occurs at relatively low supersaturations compared to that of the Form II polymorph in aqueous solution.[40] In our experiments, we would expect a similar behaviour with antisolvent addition where there will be a saturation gradient depending on the mixing of the solvent and antisolvent. We have tried to mitigate this by way of inverting the pressure cell whilst at pressure but, as can be observed in Figure 2, the ampoule is not completely shattered which would cause a concentration gradient in the vessel hence nucleation of different solid forms.

For the solution concentrations tested in the present work, no crystallization was observed in LVP experiments without antisolvent addition. This indicates that the role of the antisolvent in these experiments is either to cause crystallization upon mixing at 0.8 GPa, or that the reduction in solute solubility after mixing allows retention of a pressure-induced solid form either on compression or decompression. Further exploration of the effect of pressure on this system was performed in a DAC loaded with solutions of concentration 0.05, 0.10 and 0.20 g/g solvent mixture. As with previous testing, no nucleation was observed on compression to ca 0.8 GPa. Samples were then lowered in pressure and nucleation was observed in 0.10 and 0.20 g/g samples on decompression. For 0.05 g/g samples, it was found that taking samples to higher pressures was required to nucleate a polycrystalline product. Single crystals suitable for SC-XRD were obtained in 0.10 and 0.20 g/g samples upon in-situ nucleation (0.2g/g: Compound 1 ESI). For solids precipitated from 0.05 g/g solutions thermal and careful pressure cycling was performed to obtain a sample suitable for SC-XRD (0.79 GPa, Compound 4 ESI). In each case, the resulting solid was verified, using SC-XRD, as a MeOH solvate of PCM – not PCM I or II. From this point, samples were gradually lowered in pressure and monitored by video microscopy to determine the solubility point. One sample for each solution concentration was used to obtain an approximation of the solubility point (pressure) for the MeOH solvate crystal in the respective solutions. The MeOH solvate was seen to dissolve away completely at around 0.2 GPa on average.

During monitoring no evidence of a single crystal-single crystal transformation of the MeOH solvate was observed. During solubility determination of the crystal obtained from 0.20 g/g solution dissolution was accompanied by nucleation of a new crystal (at edge of the gasket) between 0.22-0.19 GPa (Figure

S3). The new crystal was tested by SC-XRD and verified to be PCM II (Compound 2 at 0.19 GPa & 3, ambient ESI). This observation identifies an alternative route to obtain PCM II in this system. However, if this route to PCM II occurs in the LVP experiment it would infer that anti-solvent addition at ca. 0.8 GPa leads to precipitation of the MeOH solvate that persists on decompression to around 0.21 GPa. Beyond this solubility point, dissolution of the solvate then occurs followed by nucleation of PCM II that is now recoverable to ambient pressure owing to a reduced solubility of PCM following the initial antisolvent addition.

A new solid Form

During the accompanying experiments to assess the precipitation of PCM from solution in the DAC we did not observe the precipitation of the solution to 0.8 GPa. Even with heat treatment, precipitation was not observed; this is often applied to help initiate precipitation at pressure. On decompression, however, we observed the precipitation of a solid that was stable to ca. 0.21 GPa before dissolving into solution. We were able to obtain a Raman spectrum on the precipitant as well as on an annealed single crystal; both of these spectra are consistent with one another demonstrating the single crystal is representative of the precipitated product. Single crystal diffraction data showed that this solid was a methanol solvate of paracetamol. The thrust of this study is not the identification of new phases or their relationship to each other but the process of anti-solvent addition at high pressure. Nonetheless, the structure was confirmed for each solution used albeit that not all the data were good enough to be published. We have reliable structures from crystals grown from the 0.05g/g (R_{int} 8.14%; I/σ 17.1; 9738 total reflections) and 0.2 g/g (R_{int} 7.80%; I/σ 22.0; 12334 total reflections) solutions at ~0.7 GPa. Both of these can be indexed to a larger cell (12.9717, 17.1881, 13.0437, 116.032°; $P2_1/n$, Z' = 3) than previously observed. The previous cell cannot be identified nor can integrations be performed on cells that are close to the previous work. The packing of the molecules is very similar to the previous structure with a RMS deviation of ~0.55 for the two determinations that we have made. There is a slight lateral shift in the atomic positions between the two observations. It is possible that the addition of water as part of the solvent system has played a role in the observation of this phase. Whether the difference in the solubility has altered the crystal form or whether water plays a role in the crystal structure but at a low level remains unsolved and with present technologies it is not likely to be solved. Paracetamol does form hydrated structures so the latter is not inconceivable where there is interaction with water but not in a periodic manner. Unfortunately, these observations are only observed during the DAC experiment as the large volume press does not possess windows for the observation of the solution at high-pressure. We have not observed this phase in the product from our antisolvent additions at high-pressure which indicates that either, this form is not observed at all or that it interconverts to either Form I or II of PCM on decompression, which is inferred from the images in the supplementary information (Figure S3).

Conclusions

In conclusion, we have successfully demonstrated an anti-solvent addition crystallization of a model pharmaceutical compound (paracetamol) at high-pressure conditions. Crystallization by this method allowed us to obtain a crystallised product at high-pressure and recover the form to ambient pressure due to the saturated solution after the antisolvent addition. We have also observed during the course of our investigation another solid methanol solvate of paracetamol. The observation of this new phase was limited to the compression of solutions ranging in concentration from 0.05 to 0.2 g/g PCM/solvent solution. From the decompression of this phase in a Diamond anvil cell it appears that it converts to Form II of paracetamol, which is the stable phase at high pressure compared with Form I. It is unclear, and not possible with the present experiments, whether the methanol solvate is precipitated in the anti-solvent addition experiment or whether its observation is limited to the compression of the solvent system selected. Nevertheless, we observe that the metastable Form II of paracetamol can be recovered through an antisolvent addition at high pressure. This experiment demonstrates the methodology to enable the access of thermodynamically stable forms at high pressure and the potential for them to be subsequently recovered to ambient pressure.

Conflicts of interest

There are no conflicts to declare.

Acknowledgements

IDHO & MRW thank the EPSRC for funding (EP/N015401-1). The authors would like to thank Colin Pulham (University of Edinburgh) for the data from the previous study by Fabbiani et al and Alan Kennedy (University of Strathclyde) for discussions with respect to the crystal form described in this manuscript. The authors would also like to thank Mr Michael S. P. Devlin (University of Strathclyde) for assistance with Rietveld refinements. The authors would like to acknowledge that this work was carried out in the CMAC National Facility supported by UKRPIF (UK Research Partnership Fund) award from the Higher Education Funding Council for England (HEFCE) (Grant Ref: HH13054). All data underpinning this publication are openly available from the University of Strathclyde KnowledgeBase at https://doi.org/10.15129/92b026cb-deb9-4b77-b875-717849b40fbd. CCDC deposition numbers are 1902442-1902446.

Notes and references

1 M. A. Neumann, J. van de Streek, F. P. A. Fabbiani, P. Hidber and O. Grassmann, *Nat. Commun.*, 2015, **6**, 7793.

2 R. D. L. Johnstone, A. R. Lennie, S. Parsons, E. Pidcock and J. E. Warren, *Acta Crystallogr. Sect. B Struct. Sci.*, 2009, **65**,

731–748.
3 I. D. H. Oswald, I. Chataigner, S. Elphick, F. P. A. Fabbiani, A. R. Lennie, J. Maddaluno, W. G. Marshall, T. J. Prior, C. R. Pulham and R. I. Smith, *CrystEngComm*, 2009, **11**, 359–366.
4 B. A. Zakharov, S. V Goryainov and E. V Boldyreva, *Crystengcomm*, 2016, **18**, 5423–5428.
5 M. Fisch, A. Lanza, E. Boldyreva, P. Macchi and N. Casati, *J. Phys. Chem. C*, 2015, **119**, 18611–18617.
6 B. A. Zakharov, P. A. Gribov, A. A. Matvienko and E. V. Boldyreva, *Zeitschrift für Krist. - Cryst. Mater.*, 2017, **232**, 751–757.
7 M. Ceppatelli, M. Frediani and R. Bini, *J. Phys. Chem. B*, 2011, **115**, 2173–2184.
8 R. Bini, M. Ceppatelli, M. Citroni and V. Schettino, *Chem. Phys.*, 2012, **398**, 262–268.
9 J. Guan, R. Daljeet, A. Kieran and Y. Song, *J. Phys. Condens. Matter*, 2018, **30**, 224004.
10 A. Delori, I. B. Hutchison, C. L. Bull, N. P. Funnell, A. J. Urquhart and I. D. H. Oswald, *Cryst. Growth Des.*, 2018, **18**, 1425–1431.
11 P. Á. Szilágyi, S. Hunter, C. A. Morrison, C. C. Tang and C. R. Pulham, *J. Alloys Compd.*, 2017, **722**, 953–961.
12 F. Montisci, A. Lanza, N. Casati and P. Macchi, *Cryst. Growth Des.*, 2018, **18**, 7579–7589.
13 S. A. Moggach, D. R. Allan, S. J. Clark, M. J. Gutmann, S. Parsons, C. R. Pulham, L. Sawyer and IUCr, *Acta Crystallogr. Sect. B Struct. Sci.*, 2006, **62**, 296–309.
14 H. E. Maynard-Casely, C. L. Bull, M. Guthrie, I. Loa, M. I. McMahon, E. Gregoryanz, R. J. Nelmes and J. S. Loveday, *J. Chem. Phys.*, 2010, **133**, 10.
15 N. T. Morgan, T. C. Frank, R. J. Holmes and E. L. Cussler, *Cryst. Growth Des.*, 2016, **16**, 1404–1408.
16 F. P. A. Fabbiani, C. R. Pulham and J. E. Warren, *Zeitschrift für Krist. - Cryst. Mater.*, 2014, **229**, 667–675.
17 I. D. H. Oswald and W. A. A. Crichton, *CrystEngComm*, 2009, **11**, 463–469.
18 K. W. Rajewski, I. Bukalska and A. Katrusiak, *Cryst. Growth Des.*, 2018, **18**, 3187–3192.
19 F. P. A. Fabbiani, G. Buth, D. C. Levendis and A. J. Cruz-Cabeza, *Chem. Commun. (Camb).*, 2014, **50**, 1817–9.
20 I. B. Hutchison, A. Delori, X. Wang, K. V. Kamenev, A. J. Urquhart and I. D. H. Oswald, *CrystEngComm*, 2015, **17**, 1778–1782.
21 S. Klotz, J. M. Besson, G. Hamel, R. J. Nelmes, J. S. Loveday, W. G. Marshall and R. M. Wilson, *Appl. Phys. Lett.*, 1995, **66**, 1735–1737.
22 J. M. Besson, R. J. Nelmes, G. Hamel, J. S. Loveday, G. Weill and S. Hull, *Phys. B*, 1992, **180**, 907–910.
23 N. P. Funnell, A. Dawson, W. G. Marshall and S. Parsons, *Crystengcomm*, 2013, **15**, 1047–1060.
24 C. L. Bull, N. P. Funnell, M. G. Tucker, S. Hull, D. J. Francis and W. G. Marshall, *High Press. Res.*, 2016, **36**, 493–511.
25 W. Wang, A. D. Fortes, D. P. Dobson, C. M. Howard, J. Bowles, N. J. Hughes, I. G. Wood and IUCr, *J. Appl. Crystallogr.*, 2018, **51**, 692–705.
26 C. L. Bull, N. P. Funnell, C. R. Pulham, W. G. Marshall, D. R. Allan and IUCr, *Acta Crystallogr. Sect. B Struct. Sci. Cryst. Eng. Mater.*, 2017, **73**, 1068–1074.
27 C. A. Tulk, D. D. Klug, A. M. Dos Santos, G. Karotis, M. Guthrie, J. J. Molaison and N. Pradhan, *J. Chem. Phys.*, 2012, **136**, 54502.
28 J. Abe, T. Hattori, K. Komatsu, H. Arima, M. Arakawa, A. Sano, H. Kagi, S. Harjo, T. Ito, A. Moriai, K. Aizawa, M. Arai and W. Utsumi, *J. Phys. Conf. Ser.*, 2010, **215**, 012023.
29 M. R. Ward, S. Younis, A. J. Cruz-Cabeza, C. L. Bull, N. P. Funnell and I. D. H. Oswald, *CrystEngComm*, , DOI:10.1039/C8CE01882K.
30 C. T. Ó'Ciardhá, P. J. Frawley and N. A. Mitchell, *J. Cryst. Growth*, 2011, **328**, 50–57.
31 G. J. Piermarini, S. Block, J. D. Barnett and R. A. Forman, *J. Appl. Phys.*, 1975, **46**, 2774–2780.
32 O. V. Dolomanov, L. J. Bourhis, R. J. Gildea, J. A. K. Howard, H. Puschmann and IUCr, *J. Appl. Crystallogr.*, 2009, **42**, 339–341.
33 G. Nichols and C. S. Frampton, *J. Pharm. Sci.*, 1998, **87**, 684–693.
34 F. P. A. Fabbiani, D. R. Allan, A. Dawson, W. I. F. David, P. A. McGregor, I. D. H. Oswald, S. Parsons and C. R. Pulham, *Chem. Commun. (Camb).*, 2003, **3**, 3004–3005.
35 C. F. Macrae, I. J. Bruno, J. A. Chisholm, P. R. Edgington, P. McCabe, E. Pidcock, L. Rodriguez-Monge, R. Taylor, J. van de Streek and P. A. Wood, *J. Appl. Crystallogr.*, 2008, **41**, 466–470.
36 G. M. Sheldrick, 2008.
37 A. A. Coelho, *J. Appl. Crystallogr.*, 2018, **51**, 210–218.
38 N. Al-Zoubi, J. E. Koundourellis and S. Malamataris, *J. Pharm. Biomed. Anal.*, 2002, **29**, 459–467.
39 S. C. Barthe, M. A. Grover and R. W. Rousseau, *Cryst. Growth Des.*, 2008, **8**, 3316–3322.
40 C. Sudha and K. Srinivasan, *CrystEngComm*, 2013, **15**, 1914.

Electronic Supplementary Information (ESI) – Antisolvent addition at extreme conditions

Martin R. Ward[a] and Iain D. H. Oswald[a]

[a]*Strathclyde Institute of Pharmacy & Biomedical Sciences (SIPBS), University of Strathclyde, 161 Cathedral Street, Glasgow, G4 0RE, UK.*

S1. Large volume press (LVP)

The LVP used in this work is of the same construction as reported previously. For antisolvent addition, a glass tube was designed to hold the selected antisolvent (water). The length of the glass tube was specific to the target pressure that we wished the tube to break. Tests were performed to measure the contraction of the sample tube as a function of applied load (See Section S4). The glass tube was prepared by flame sealing a standard laboratory glass pipette approximately 25 mm from the taper (Figure S1). After cooling, the remaining piece was cut to the desired size using a ceramic cutting blade before filling with deionized water using a syringe and needle. Once filled, the antisolvent tube was sealed using epoxy glue and allowed to fully harden before use in LVP experiments. The length of the resulting sealed tube was verified to be suitable prior to experiment after checking of the sealed tube length and the length of the PTFE sample tube. Prior to use in LVP experiment, the glass tube was lightly scored around the diameter of the tube to promote breakage at the target pressure.

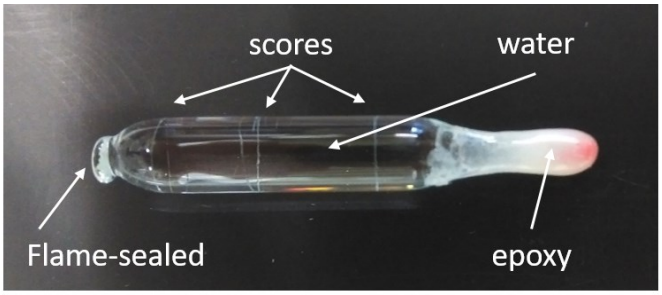

Figure S1. Prepared antisolvent glass tube. Glass tube formed by flame-sealing a laboratory glass pipette and then cutting the pulled tip to size before filling and sealing with epoxy glue

S2. UV-vis concentration determination

Spectra were obtained over the range 200-400 nm and the absorbance at 248 nm used for evaluation of PCM concentration. In order to avoid saturation of the spectrograph detector it was found that 0.2 g/g solutions required dilution by a factor of 8000 – this dilution factor was applied to all measured samples. A calibration curve was produced using standard samples of PCM dissolved in 64% w/w MeOH:H_2O with concentrations of 0.14, 0.16, 0.18, 0.20 and 0.22 g/g. A plot of the calibration curve is shown in Figure S2.

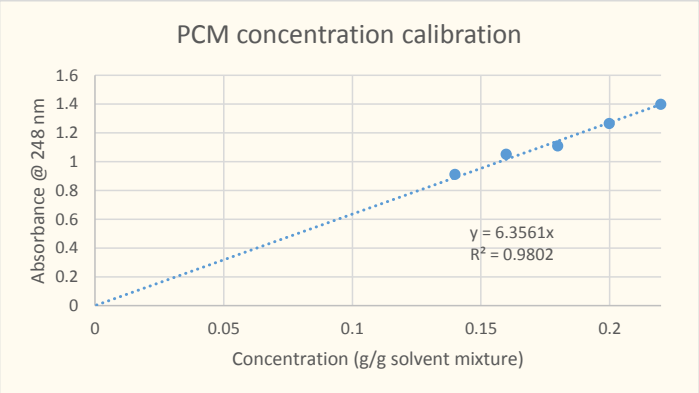

Figure S2. Calibration curve obtained for standard PCM solutions prepared in 64% w/w MeOH:H_2O. Dotted line shows the linear line of best fit with y-intercept = 0.

The solute concentration in samples following LVP compression were tested by pipetting 5 ul and diluting by a factor of 8000 with 64% w/w MeOH:H_2O solvent mixture. 3.0 mL of diluted sample was transferred to a 10 mm pathlength quartz glass cuvette for UV-vis measurement. Each sample concentration was measured in triplicate and averaged to obtain the mean absorbance for each concentration. A summary of the PCM concentration in the top portion of samples after compression/decompression in LVP (without antisolvent addition) is shown in Table S1

Table S1. Summary of PCM concentrations in upper layer of solution sample after compression/decompression in large volume press experiment determined UV-vis.

Solution concentration (g/g solvent)	Mean absorbance (248 nm)	Calculated concentration (g/g solvent)	% difference to expected concentration
0.14	0.302	0.048	66.0
0.16	0.446	0.070	56.1
0.18	0.631	0.099	44.9
0.20	0.682	0.107	46.4
0.22	0.973	0.153	30.4

S3. SC-XRD testing

S3.1 DAC samples

A Merrill-Basset DAC (600 um culet diamonds) was used with an indented tungsten foil gasket (100 um thick) that was drilled to prepare a 250 um hole for the sample chamber. Solution samples were loaded along with a small chip of ruby to provide pressure readout by the ruby fluorescence method.[1] Solution samples were taken to approximately 0.8 GPa to achieve comparable pressures to those in the LVP experiment. Crystal nucleation was only observed on decrease of pressure from this point (0.10 and 0.20 g/g solution samples) and on the application of further pressure to ca. 1.5 GPa for 0.05 g/g solution sample.

Crystals obtained by in-situ nucleation experiments were subject to single crystal X-ray diffraction (SC-XRD) to verify the solid form. Data were collected using a standard run list as shown in Table S2.

Table S2. Typical data collection strategy used for DAC samples. Frame exposure time can vary depending on the nature (quality/size) of the sample crystal

Scan	distance (mm)	2 Theta (deg)	Omega (deg)	Phi (deg)	Chi (deg)	Time (sec)	Width (deg)	Sweep (deg)	direction
Omega	70	-28	-10	0	54.726	30	0.3	30	negative
Omega	70	28	40	0	54.726	30	0.3	65	negative
Omega	70	-28	25	0	-54.726	30	0.3	65	negative
Omega	70	28	40	0	-54.726	30	0.3	30	negative
Omega	70	-28	-10	180	54.726	30	0.3	30	negative
Omega	70	28	40	180	54.726	30	0.3	65	negative
Omega	70	-28	25	180	-54.726	30	0.3	65	negative
Omega	70	28	40	180	-54.726	30	0.3	30	negative
Omega	70	28	40	0	90	30	0.3	52	negative
Omega	70	-28	29	0	-90	30	0.3	64	negative
Omega	70	28	40	180	90	30	0.3	52	negative
Omega	70	-28	29	180	-90	30	0.3	64	negative

Owing to the quality of the in-situ grown crystals, a few runs were sufficient for indexing of crystals. Several full collections were performed on samples that were later identified as a PCM:MeOH solvate. Data for these samples were reduced using Bruker, Apex3 software. Resolved structures were solved by intrinsic phasing using SHELXT using Olex2 (v1.2) software. Full-matrix least-squares refinement of data was also performed with SHELXL using Olex2 software. All non-hydrogen atoms were treated anisotropically for the Form II whilst for the methanol solvate the non-hydrogen atoms were treated isotropically due to the paucity of data. Hydrogen atoms were placed on the carbon atoms and allowed to ride on their parent atoms. The datasets from the 0.1g/g PCM solutions were not of sufficient quality to be deposited in the Cambridge Structural Database but were submitted as part of the reviewing process.

Details of the DAC samples that were tested by SC-XRD are provided in Table S3 and their crystallographic information can be found in Table S4.

Table S3. Summary of XRD data collection performed for samples in DAC.

Compound	Sample	Solution concentration (g PCM / g solvent mixture)	Pressure (GPa)	Solid form	CCDC code
	PCM_01gg_201218	0.1	0.76	MeOH:PCM	-
	PCM_01gg_040119	0.1	0.76	MeOH:PCM	-
1	PCM_02gg_070119	0.2	0.71	MeOH:PCM	1902446
2	PCM_02gg_180119	0.2	0.19	PCM II	1902444
3	PCM_02gg_ambient	0.2	Ambient	PCM II	1902442
4	PCM_005gg_250119	0.05	0.79	MeOH:PCM	1902445

Table S4: Crystallographic information for the five datasets taken at various solution concentrations and pressures. Dataset 1 crystallised from a 0.2 g/g paracetamol to methanol:water (64% w/w) solution at 0.72 GPa. Dataset 2 was performed on a crystal isolated from same loading as 1 but reduced in pressure to 0.21 GPa. The crystal grew from solution (FigureS3) after leaving the sample. Dataset 3 was the same crystal as dataset 2 but at ambient pressure. Dataset 4 was taken on a crystal isolated from a 0.05 g/g paracetamol to methanol:water (64% w/w) solution at 0.75 GPa. Dataset 5 was taken on a crystal at ambient pressure recovered from the large volume press.

	(1)	(2)	(3)	(4)	(5)
Crystal data					
Chemical formula	$CH_4O{\cdot}C_8H_9NO_2$	$C_8H_9NO_2$	$C_8H_9NO_2$	$CH_4O{\cdot}C_8H_9NO_2$	$C_8H_9NO_2$
M_r	183.20	151.16	151.16	183.20	151.16
Crystal system, space group	Monoclinic, $P2_1/n$	Orthorhombic, *Pbca*	Orthorhombic, *Pbca*	Monoclinic, $P2_1/n$	Orthorhombic, *Pbca*
Temperature (K)	293	296	296	293	296
Pressure (GPa)	0.72	0.21	Ambient	0.75	Ambient
a, b, c (Å)	13.0234 (15), 17.2078 (9), 13.0925 (15)	17.1202 (17), 11.7968 (11), 7.288 (2)	17.143 (8), 11.806 (6), 7.399 (10)	12.9717 (15), 17.1881 (9), 13.0437 (19)	17.1522 (5), 11.8201 (4), 7.3985 (2)
α, β, γ (°)	90, 116.209 (7), 90	90, 90, 90	90, 90, 90	90, 116.032 (8), 90	90, 90, 90
V (Å^3)	2632.4 (5)	1471.9 (5)	1497 (2)	2613.2 (5)	1499.98 (8)
Z	12	8	8	12	8
Radiation type	Mo $K\alpha$	Mo $K\alpha$	Mo $K\alpha$	Mo $K\alpha$	Cu $K\alpha$
μ (mm^{-1})	0.10	0.10	0.10	0.11	0.80
Crystal size (mm)	0.15 × 0.14 × 0.05	0.09 × 0.07 × 0.05	0.09 × 0.07 × 0.05	0.18 × 0.06 × 0.05	0.2 × 0.18 × 0.05
Data collection					
Diffractometer	Bruker *APEX*-II CCD	Bruker *APEX*-II CCD	Bruker *APEX*-II CCD	Bruker *SMART APEX2* area detector	Bruker *APEX*-II CCD
Absorption correction	Multi-scan *SADABS2016*/2 (Bruker,2016/2) was used for absorption correction. wR2(int) was 0.1071 before and 0.0616 after correction. The Ratio of minimum to maximum transmission is 0.8490. The λ/2 correction factor is Not present.	Multi-scan *SADABS2016*/2 (Bruker,2016/2) was used for absorption correction. wR2(int) was 0.1466 before and 0.0755 after correction. The Ratio of minimum to maximum transmission is 0.8510. The λ/2 correction factor is Not present.	Multi-scan *SADABS2016*/2 (Bruker,2016/2) was used for absorption correction. wR2(int) was 0.0969 before and 0.0605 after correction. The Ratio of minimum to maximum transmission is 0.7071. The λ/2 correction factor is Not present.	Multi-scan *SADABS2016*/2 (Bruker,2016/2) was used for absorption correction. wR2(int) was 0.0848 before and 0.0556 after correction. The Ratio of minimum to maximum transmission is 0.9145. The λ/2 correction factor is Not present.	Multi-scan *SADABS2016*/2 (Bruker,2016/2) was used for absorption correction. wR2(int) was 0.0894 before and 0.0482 after correction. The Ratio of minimum to maximum transmission is 0.8688. The λ/2 correction factor is Not present.
T_{min}, T_{max}	0.632, 0.745	0.634, 0.745	0.527, 0.745	0.681, 0.745	0.654, 0.753
No. of measured, independent and observed [$I >$	12022, 1214, 819	4019, 413, 271	866, 304, 161	9591, 1319, 765	15062, 1378, 1223

$2\sigma(I)$] reflections					
R_{int}	0.078	0.118	0.129	0.081	0.038
θ_{max} (°)	23.3	23.3	23.4	23.3	68.3
$(\sin\theta/\lambda)_{max}$ (Å^{-1})	0.556	0.557	0.558	0.556	0.603
Refinement					
$R[F^2 > 2\sigma(F^2)]$, $wR(F^2)$, S	0.094, 0.272, 1.07	0.058, 0.147, 1.08	0.068, 0.207, 1.08	0.129, 0.417, 1.55	0.045, 0.122, 1.07
No. of reflections	1214	413	304	1319	1378
No. of parameters	130	90	90	130	91
No. of restraints	0	75	75	0	75
$\Delta\rangle_{max}$, $\Delta\rangle_{min}$ (e Å^{-3})	0.31, -0.23	0.13, -0.15	0.14, -0.13	0.56, -0.36	0.30, -0.18

S3.2 Ambient pressure PCM II

Following LVP experiments, the sample material recovered was tested by SC-XRD to verify its contents. Crystals were dispersed in silicone oil and mounted on a low-background Kapton microloop (200 µm). Data was collected on a Bruker D8 Venture diffractometer equipped with a Photon 100 detector. Crystals were indexed in order to assess their solid form, in order to do this a 'fast scan' experimental method was employed. This method is also used for screening crystals ahead of determining the strategy for a full collection for structural solution.

A full collection was performed on a particle of PCM II in order to assess the quality of the crystallized material. A summary of the collected data is shown in **Error! Reference source not found.** Compound 5.

S4. Axial compression measurement

For large volume press antisolvent experiments it was necessary to establish the resulting length of the PTFE tube as a function of pressure. This would in turn allow us to produce a glass tube of suitable length such that it breaks at the target pressure (internal length of the PTFE sample tube). Contraction of the sample tube was monitored by video microscopy during compression of 2 solvent systems – water and methanol:water (64% w/w).

PTFE sample tubes were assembled as per normal procedures and filled only with the chosen solvent before capping and assembling in the copper beryllium cell. Sample pressure is generated by use of a pneumatic actuator to apply load to the top of the sample tube. A camera (Basler acA1920—40uc) and zoom lens was used to image the actuator and to monitor its translation as a function of applied load. Still images were obtained at each pressure point and analysed using ImageJ to calculate the translation of the actuator.

S5. Video monitoring

Video monitoring of DAC samples was performed using solution concentrations of 0.05, 0.10 and 0.20 g/g PCM/solvent mixture. Solution samples were loaded in a DAC for compression and decompression studies. Video microscope was used to monitor crystallized material during decompression to aid identification of the dissolution point of the crystalline phase

S5.1 Dissolution point monitoring

Once a sample had nucleated and a suitable crystal was obtained the sample pressure was gradually decreased and monitored at each point by video microscopy. Sample pressure was established by the ruby fluorescence technique using an Almax Optiprexx PLS spectrometer equipped with a 532 nm

excitation laser (20 mW). At each pressure point the sample would be monitored over at least a 30 minute period with images recorded every minute. For longer monitoring periods (over night or weekend during experiments) a 5 minute or 30 minute interval would be used.

Table S4. Summary of dissolution points (pressure) recorded for PCM:MeOH solvate in solutions of 0.05, 0.10 and 0.20 g/g concentration in 64% w/w MeOH:H2O solvent mixture.

Solution Concentration (g/g solvent)	Lowest pressure crystal observed (GPa)	Highest pressure solution phase (GPa)
0.05	0.30	0.26
0.10	0.14	0.13
0.20	0.22	0.19

For each sample concentration the pressure at which the crystal completely dissolved was recorded. Only one sample was used for this determination for each of the solution concentrations, the obtained solubility points are summarized in Table S4.

S5.2 Nucleation of PCM II

During monitoring of the 0.2 g/g sample dissolution of a MeOH solvate crystal (verified by SC-XRD) was observed and simultaneously nucleation of a crystal at the gasket edge was observed. This process is summarized in Figure S3a-d that shows frames during the transformation over a 4-hour period. The nucleated crystal was subsequently identified as PCM II by SC-XRD (Table S4; 2)

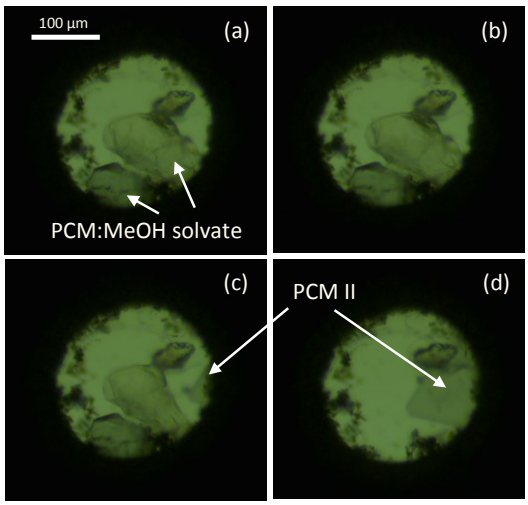

Figure S3. Still images taken from video monitoring of MeOH solvate in 0.2 g/g solution at ca. 0.21 GPa. The consecutive frames are recorded every 30 minutes and show the dissolution of PCM:MeOH and the nucleation and growth of a new crystal subsequently identified as PCM II by SC-XRD (compound 2). The scale bar in the image represents 100 µm.

Commented [MW1]: For Editor

Table labelling corrected

S5.3 Solution mediated transformation (PCM II -> I)

Following a LVP antisolvent addition experiment, sample was taken immediately for monitoring using a Leica DM6000M microscope. Solids were not isolated from the supernatant but were left in the mother liquor to monitor for suspected solution mediated phase transformation. The sample was monitored over a 30 minute period with an image recorded every 60 seconds. The recorded images show dissolution of PCM II (needles) and simultaneous growth and nucleation of PCM I (blocks), Figure S4. An animated version of this timelapse, which show the transformation more clearly, are available in the ESI for this paper.

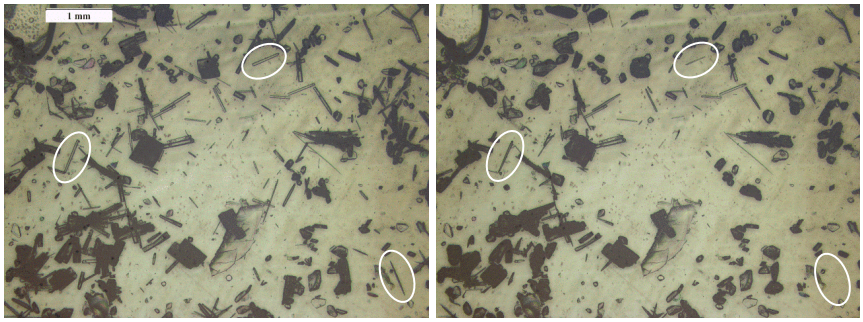

Figure S4. The first and last image recorded during a 30 minute monitoring period of the sample material obtained from LVP experiment. The particles were not isolated from the supernatant, but remain in contact with the solution phase. Images were recorded every 60 seconds and show the rapid dissolution of PCM II particles (rods) and growth of PCM I (blocks). The scale bar represents 1 mm. Dissolution of PCMII particles has been highlighted (white circle)

S6. X-ray powder diffraction

XRPD data was collected on samples isolated after LVP antisolvent addition experiment. The same sample was repeatedly collected 5 times over 3 hours (approx. 35 min/collection). The XRPD patterns obtained in this test are shown in Figure S5. The patterns show no change with time and indicate that after isolation from the supernatant, no further solid form change occurs (over a monitoring period on XRPD of ca 3 hours).

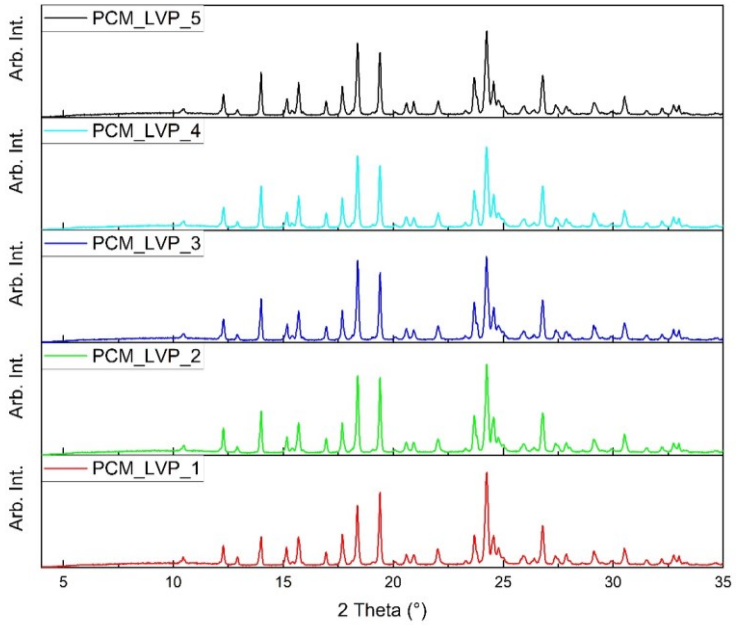

Figure S5. XRPD patterns obtained from the same sample after isolation from the supernatant following LVP experiment. Each pattern was recorded over a 35 minute period and no change in pattern is observed.

The same sample was then collected over a longer period (7 hours) to obtain a pattern with improved signal:background for Rietveld refinement. The XRPD pattern obtained is shown in Figure S6. This pattern is again unchanged from the pattern first obtained after isolation of the sample and therefore demonstrates that the isolated sample remains unchanged for at least 10 hours once removed from the supernatant.

With a view to investigating the role of solution mediated transformation of PCM II → PCM I, the LVP anti-solvent addition experiment was performed with 0.5 mL of perfluorinated oil (Perfluoropolyether fluid, Galden SV110, Solvay, Italy) in the sample tube. The aim of this was to establish if precipitated particles could be 'protected' from the solution phase by being trapped in or by being coated by the hydrophobic oil phase. Solids isolated from this test were tested by XRPD, the obtained pattern is shown in Figure S6.

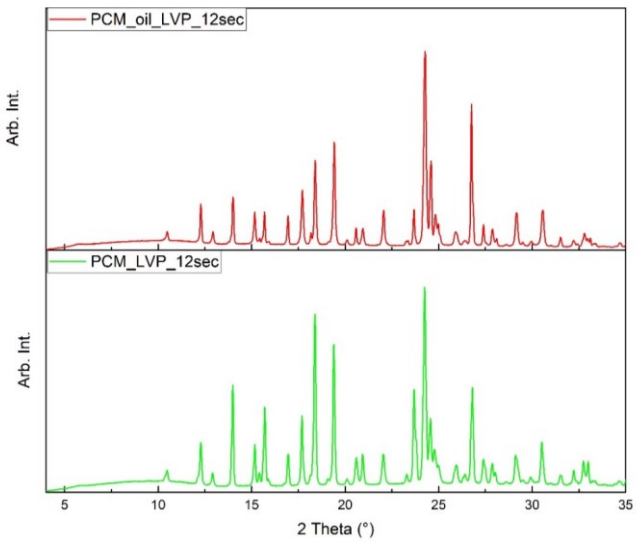

Figure S6. XRPD patterns obtained from samples produced by LVP experiment with (upper, red) and without (lower, green) inclusion of 500 µl perfluorinated oil. Subtle difference in the patterns indicate differences in the relative amounts of PCM I and II in the sample mixtures.

Analysis of the patterns by Rietveld refinement (performed using Topas 5.0 academic version[2]) show an increased proportion of PCM II in the test performed using oil. Reference structures for PCM I and II were retrieved from the CSD database[3] (HXACAN04[4] and HXACAN08[5]) and used for refinement. Plots showing the output of Rietveld refinement for samples obtained without and with oil in LVP experiment are shown in Figure S7 and Figure S8, respectively.

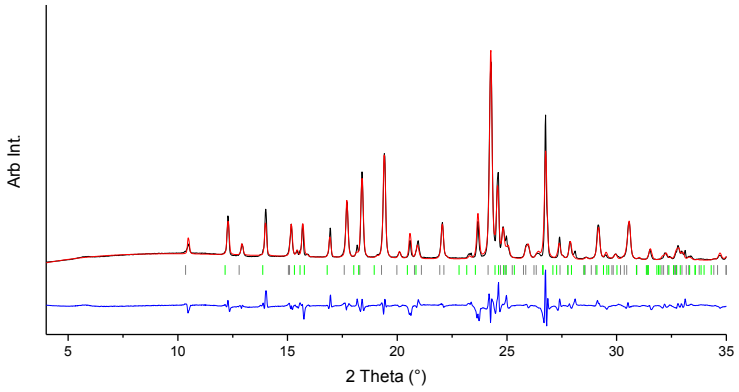

Figure S7. Results plot from Rietveld refinement of XRPD data obtained in LVP experiment without use of perfluorinated oil. Rietveld refinement indicates ca. 58 % content of PCM II in the sample mixture. Experimental data is represented by the black line, fitted data shown by the red line and the difference shown in blue. Green and grey tick marks represent reflections attributed to PCM forms I and II, respectively.

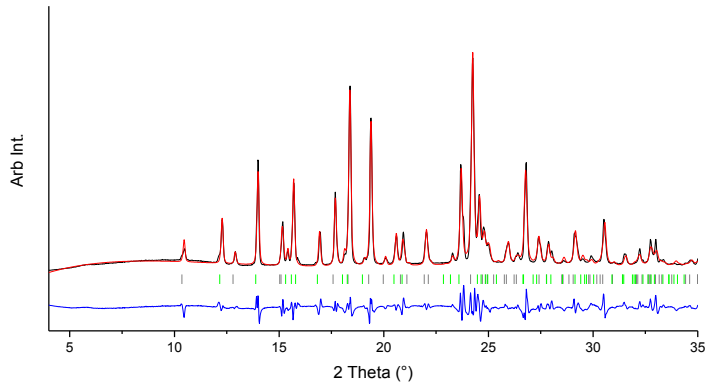

Figure S8. Results plot from Rietveld refinement of XRPD data obtained in LVP experiment without use of perfluorinated oil. Rietveld refinement indicates ca. 65 % content of PCM II in the sample mixture. Experimental data is represented by the black line, fitted data shown by the red line and the difference shown in blue. Green and grey tick marks represent reflections attributed to PCM forms I and II, respectively.

S7. Raman spectra, MeOH solvate

As part of characterization of the identified MeOH solvate of PCM, Raman spectrum was collected of the crystal obtained from 0.05 g/g solvent mixture (64:36 w/w, MeOH:H_2O). The recorded spectrum is shown in Figure S9.

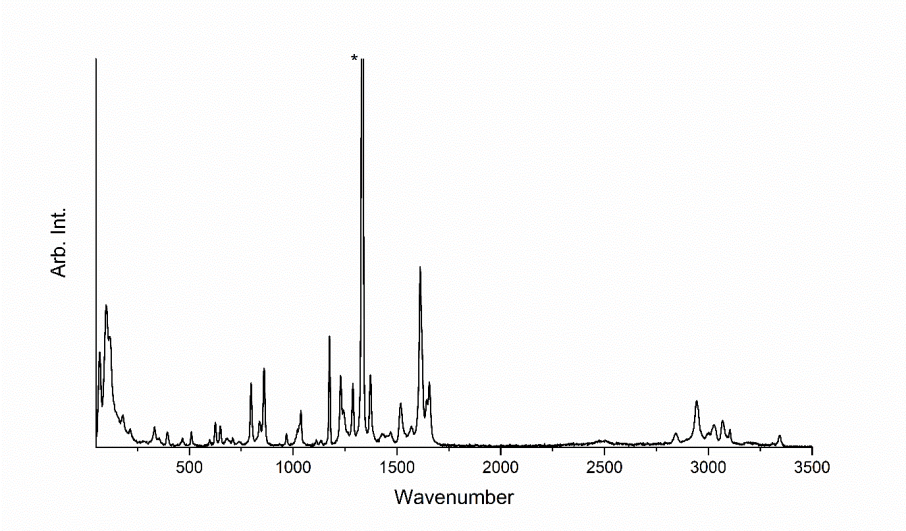

Figure S9. Raman spectrum obtained from MeOH solvate of PCM obtained from 0.05 g/g solvent mixture solution at 0.2 GPa in diamond anvil cell. Peak at approx. 1330 cm^{-1}, marked with asterisk, attributed to diamond.

References:

1 G. J. Piermarini, S. Block, J. D. Barnett and R. A. Forman, *J. Appl. Phys.*, 1975, **46**, 2774–2780.

2 A. Coelho, *TOPAS – Acad. Gen. Profile Struct. Anal. Softw. Powder Diffr. Data*, 2012.

3 C. R. Groom, I. J. Bruno, M. P. Lightfoot and S. C. Ward, *Acta Crystallogr. Sect. B*, 2016, **72**, 171–179.

4 D. Y. Naumov, M. A. Vasilchenko, J. A. K. Howard and IUCr, *Acta Crystallogr. Sect. C Cryst. Struct. Commun.*, 1998, **54**, 653–655.

5 G. Nichols and C. S. Frampton, *J. Pharm. Sci.*, 1998, **87**, 684–693.